Journal of Molecular Structure: THEOCHEM 943 (2010) 65–70

Contents lists available at ScienceDirect

Journal of Molecular Structure: THEOCHEM

journal homepage: www.elsevier.com/locate/theochem

Variations in electron density and bonding in the lowest $^1\Sigma_g$ state of H_2 molecule under strong magnetic fields by using a time-dependent density functional theory

Mainak Sadhukhan, B.M. Deb *

Department of Chemical Sciences, Indian Institute of Science Education & Research, Mohanpur Campus, Post Office BCKV Main Campus, Mohanpur, 741252 West Bengal, India

ARTICLE INFO

Article history:
Received 30 July 2009
Received in revised form 17 October 2009
Accepted 18 October 2009
Available online 23 October 2009

Dedicated to Dr. Swapan K. Ghosh on his 60th birthday.

Keywords:
Strong magnetic fields
Bonding in H_2 molecule
Bond-shortening

ABSTRACT

The mechanism of decrease of bond length and the shifting of electronic cusps corresponding to nuclear positions under strong magnetic fields (up to 2.3505×10^9 G) in the lowest $^1\Sigma_g$ state ($M = 0$) of the H_2 molecule is studied by means of a time-dependent density functional equation. The applied magnetic field along the internuclear axis imparts to the electrons an additional motion, resulting in an excess rotational kinetic energy, transverse to the direction of the field. As a result, the electron density contracts towards the internuclear axis, leading to a flow of density from the anti-binding regions behind the nuclei to the binding region between the two nuclei. The consequent shortening of the bond length and the inward shifting of electronic cusps make the molecule more stable even though the overall electronic energy increases as a result of increased kinetic energy. The overall phenomenon may be looked at in terms of a competition between the nuclear electric field and the external magnetic field, which is mainly responsible for the detailed changes in the electron density.

1. Introduction

The nature of the chemical bond under extreme conditions of intense electric fields and/or strong magnetic fields has been a subject of considerable recent interest [1–6]. In the case of electric fields from intense laser sources, it is now understood that a diatomic molecule dissociates by Coulomb explosion [1]. This occurs due to the creation of positive charges on the two molecular fragments which results from the following effects: (i) Ionization [1,4], (ii) movement of electron density away from the binding region between the two nuclei [4], and (iii) movement of electron density to the anti-binding regions behind the two nuclei, thereby partially de-shielding them from each other, weakening the bond and increasing the repulsion between the two nuclei [4]. Theoretical studies on molecules under intense laser electric fields have employed both wave function-based and density-based time-dependent approaches [1–4].

More recently, there has also been significant interest in examining the H_2 molecule (a prototype of the two-electron bond) under strong magnetic fields, of strengths 10^9 G and greater, which occur on the surfaces of pulsars, white dwarfs and neutron stars [7] (for H_2^+ molecule-ion in strong magnetic fields, see [8,9]). Issues addressed under strong magnetic fields have been the following: (i) Can hydrogen gas undergo Bose–Einstein condensation into a superfluid [10]? The answer at present is negative [11]. (ii) Can new covalent bonds be formed between atoms which otherwise do not bond together [5]? The answer to this is not known. (iii) Changes in mesoscopic structures, e.g., edge reconstruction in quantum dots [12]. (iv) Condensation of atoms and formation of chain molecules [13]; this too has not been studied. (v) The ascertaining of the nature and symmetry of the ground state of molecules under different field strengths [14–18]. In a detailed work, by using a basis set of non-orthogonal, non-spherical Gaussian orbitals within a wave function-based CI approach, it was found by Detmer et al. [15,16] that as the strength of the magnetic field *parallel to the internuclear axis* increases, the ground state of the H_2 molecule changes first from the strongly bound $^1\Sigma_g$ state to the unbound $^3\Sigma_u$ state and then, as the magnetic field rises further, to the strongly bound $^3\Pi_u$ state. In other words, the space and spin symmetries of the ground state change depending on the strength of the magnetic field. The potential energy curves, in varying magnetic fields, for the $^1\Sigma_g$, $^3\Sigma_g$, $^1\Sigma_u$, $^3\Sigma_u$, $^1\Pi_g$, $^3\Pi_g$, $^1\Pi_u$ and $^3\Pi_u$ states as well as changes in dissociation energy and equilibrium internuclear distance (R_{eq}) have also been calculated [14–18]. In particular, for the $^1\Sigma_g$ state, R_{eq} decreases and the dissociation energy increases with increase in magnetic field strength.

In this paper, we report what appears to be the first density functional study on H_2 molecule in strong magnetic fields, using the Deb–Chattaraj generalized non-linear Schrödinger equation

* Corresponding author. Tel.: +91 033 23355706; fax: +91 33 23348092.
E-mail address: bmdeb@yahoo.co.in (B.M. Deb).

0166-1280/$ - see front matter © 2009 Elsevier B.V. All rights reserved.
doi:10.1016/j.theochem.2009.10.021

[19] based on the net time-dependent (TD) spinless density. This equation employs a fluid dynamical analogy [20,21] which led to the formulation of TD density functional theory in absence and presence of external fields [22–25]. Since the net density is totally symmetric, it does not admit the use of group theory and therefore the present approach will not be able to detect the $^1\Sigma_g \rightarrow {}^3\Sigma_u \rightarrow {}^3\Pi_u$ state transitions with progressive increases in field strength, unless a hybrid density–wave function-based approach is employed. Furthermore, in the Deb–Chattaraj formulation [19] of the single TDDFT equation for a many-particle system, a rotational contribution was neglected, which may cause significant error at very strong magnetic fields. For these reasons, in this exploratory study, complementary to the earlier works described above, we follow the evolution of only the lowest $^1\Sigma_g$ state from zero magnetic field up to a field strength of 2.3505×10^9 G. The transparency and direct physical interpretability associated with the single-particle density allows us to obtain additional insights into the mechanism of bond strengthening in terms of the spatial changes in electron density under strong magnetic fields.

In Section 2 we present the approach to the problem. Section 3 discusses the results while Section 4 draws certain conclusions.

2. Formulation

In this section, we develop a single density equation for a many-electron system in time-dependent as well as time-independent magnetic fields. We begin with the Schrödinger representation in which the operators are time-independent while the wave function or probability density is time-dependent. Later, we will adopt an intermediate representation in which the operators and probability density are both time-dependent.

Consider the N-electron, time-dependent Schrödinger equation.

$$\hat{H}\Psi(\mathbf{r}_1, \mathbf{r}_2, \ldots\ldots, \mathbf{r}_N, t) = i\hbar\, \partial\Psi(\mathbf{r}_1, \mathbf{r}_2, \ldots\ldots, \mathbf{r}_N, t)/\partial t \tag{1}$$

where $\hat{H}$ is the many-electron, spinless Hamiltonian,

$$\hat{H} = \sum_j (\mathfrak{p}_j + e\mathbf{A}_j/c)^2/2m + \sum_{i<j} V(r_{ij}) \tag{2}$$

with $\mathfrak{p}_j = -i\hbar\, \nabla_j$ as the momentum operator for the jth electron, $\mathbf{A}_j \equiv \mathbf{A}_j(\mathbf{r}_j, t)$ as the vector potential on the jth electron, e as the magnitude of electronic charge, m as the electronic mass and c as the speed of light.

One can partition the Hamiltonian in terms of a non-magnetic and a magnetic term as

$$\hat{H} = \hat{H}_0 + \hat{H}_m$$

where the non-magnetic term on the right-hand side is given by

$$\hat{H}_0 = \sum_j (-\hbar^2/2m)\nabla_j^2 + \sum_{i<j} V(r_{ij}) \tag{3}$$

and the magnetic term can be written as

$$\hat{H}_m = (e^2/2mc^2)\sum_j \mathbf{A}_j^2 - (ei\hbar/2mc)\sum_j (\mathbf{A}_j \cdot \nabla_j + \nabla_j \cdot \mathbf{A}_j) \tag{4}$$

Using the transverse gauge condition, i.e., taking the magnetic field along the z-direction and by exploiting the cylindrical symmetry of the system, we have

$$\sum_j (\nabla_j \cdot \mathbf{A}_j) = 0 \tag{5}$$

$$\mathbf{A}_j = (y_j\mathbf{e}_x - x_j\mathbf{e}_y)B_z/2 \tag{6}$$

where B_z is the z-component of the magnetic field B (here $B_z = B$); the magnetic field may be time-dependent or time-independent. Hence, Eq. (4) now gives

$$\hat{H}_m = (e^2/2mc^2)\sum_j \mathbf{A}_j^2 - (ei\hbar/2mc)\sum_j \mathbf{A}_j \cdot \nabla_j \tag{7}$$

The total energy under the magnetic field is likewise a sum of non-magnetic and magnetic components E_0 and E_m, where.

$$E_0 = \langle\Psi|\hat{H}_0|\Psi\rangle$$

$$E_m = \langle\Psi|\hat{H}_m|\Psi\rangle$$

Both E_0 and E_m can be expressed in terms of the net TD electron density $\rho(\mathbf{r}, t)$. E_0 has been analyzed earlier [19,22]. E_m can also be written as a sum of two terms, viz.,

$$E_m = (e^2/2mc^2)\left\langle \Psi \middle| \sum_j \mathbf{A}_j^2 \middle| \Psi \right\rangle - (ei\hbar/2mc)\left\langle \Psi \middle| \sum_j \mathbf{A}_j \cdot \nabla_j \middle| \Psi \right\rangle \tag{8}$$

Since $\mathbf{A}_j^2$ depends only on single-particle coordinates, the first term (say, E_m^1) on the right-hand side of Eq. (8) becomes, by using Eq. (6) and integrating with respect to the coordinates of all but one electron,

$$E_m^1 = (e^2B_z^2/8mc^2)\int d\mathbf{r}\ \rho(\mathbf{r}, t)(x^2 + y^2) \tag{9}$$

The second term (say, E_m^{int}) on the right-hand side of Eq. (8) vanishes for stationary states. Note that, since Ψ is time-dependent, E_0, E_m, E_m^1 and E_m^{int} are all time-dependent. Therefore, in a dynamical situation, they are not observables. They become observables when Ψ is a stationary state and the operator is time-independent.

The vanishing of E_m^{int} is shown below in two different ways: (1) One recognizes that $\sum_j \mathbf{A}_j \cdot \nabla_j$ is proportional to $\sum_j \mathbf{L}_j \cdot \mathbf{B}$, where $\mathbf{L}_j$ is the jth electronic orbital angular momentum. Since $\mathbf{B} = B_z\mathbf{e}_z$, one can write $B_z\sum_j \mathbf{L}_j = B_z\mathbf{L}_z$, where $\mathbf{L}_z = \sum_j \mathbf{L}_{jz}$ is the total orbital angular momentum operator. Now, let

$$\mathbf{L}_z|\Psi\rangle = \hbar\, M|\Psi\rangle \tag{10}$$

where Ψ is a stationary state and M is the quantum number corresponding to the z-component of total angular momentum. By choosing to work only with the unperturbed ground $^1\Sigma_g$ state for which we adopt $M = 0$, even in presence of a magnetic field, the second term is made to vanish. Therefore, for stationary states having $M = 0$, one obtains

$$E_m = E_m^1 = (e^2B_z^2/8mc^2)\int d\mathbf{r}\ \rho(\mathbf{r})(x^2 + y^2) \tag{11}$$

where $\rho(\mathbf{r}, t)$ in Eq. (9) is replaced by $\rho(\mathbf{r})$ for stationary states.

(2) Write the time-dependent wave function as a many-electron hydrodynamical function as

$$\Psi(\mathbf{r}_1, \mathbf{r}_2, \ldots\ldots, \mathbf{r}_N, t) = \psi(\mathbf{r}_1, \mathbf{r}_2, \ldots\ldots, \mathbf{r}_N, t) \times \exp(i\, S(\mathbf{r}_1, \mathbf{r}_2, \ldots\ldots, \mathbf{r}_N, t)/\hbar) \tag{12}$$

where ψ and S are time-dependent real functions. In view of the cylindrical symmetry of the system, one can write

$$\int \mathrm{d}x\ \mathrm{d}y\ \mathrm{d}z\ x^2 f(x, y, z) = \int \mathrm{d}x\ \mathrm{d}y\ \mathrm{d}z\ y^2 f(x, y, z) \tag{13a}$$

$$\int \mathrm{d}x\ f(x, y, z) = \int \mathrm{d}y\ f(x, y, z) \tag{13b}$$

where $f(x, y, z)$ is a function with cylindrical symmetry. Thus, one can now write

$$E_m^{int} = (ei\hbar/mc)\sum_j \int d\mathbf{r} \int d\mathbf{r}_2 d\mathbf{r}_3 \ldots\ldots d\mathbf{r}_N \mathbf{A}_j \cdot \nabla_j \psi^2 - (2e/mc)\sum_j \int d\mathbf{r} \int d\mathbf{r}_2 d\mathbf{r}_3 \ldots\ldots d\mathbf{r}_N \psi^2 \mathbf{A}_j \cdot \nabla_j S \tag{14}$$

One can show that each of the two terms on the right-hand side of Eq. (14) vanishes separately. Therefore, E_m^{int} vanishes and this again yields Eq. (11). Hence, following the early work by Deb and Ghosh [22], one now obtains a new density functional $h[\rho]$, given by

$$\int d\mathbf{r}\, h[\rho] = \int d\mathbf{r}\Big\{G[\rho] + \int d\mathbf{r}'\rho(\mathbf{r},t)\rho(\mathbf{r}',t)/|\mathbf{r}-\mathbf{r}'| + v_{ext}(\mathbf{r},t)\rho(\mathbf{r},t) + (e^2B_z^2/8mc^2)\rho(\mathbf{r},t)(x^2+y^2)\Big\} \quad (15)$$

where the last term is the magnetic potential energy. Now, define a dimensionless parameter $\beta = B_z/B_0$, where $B_0 = 4.7010 \times 10^9$ G [11], such that $e^2B_z^2/8mc^2$ becomes $\beta^2/2$ in a.u. Then, the magnetic potential term of Eq. (15) becomes $\beta^2\,(x^2+y^2)/2$, causing an extra motion (analogous to the ponderomotive potential in the case of intense laser-atom interaction) of electron density in a plane perpendicular to the direction of the applied magnetic field. Therefore, the Deb–Chattaraj equation [19] now becomes (*in a.u. which will be employed henceforth*) the following single-particle equation in which two-particle quantum effects such as exchange and correlation are built in.

$$[-\nabla^2/2 + V_{eff}(\rho;\mathbf{r},t)]\;\Phi(\mathbf{r},t) = i\partial\Phi(\mathbf{r},t)/\partial t \quad (16)$$

where $\Phi(\mathbf{r}, t)$ is the single-particle hydrodynamical function, with $|\Phi(\mathbf{r}, t)|^2 = \rho(\mathbf{r}, t)$. $V_{eff}(\rho; \mathbf{r}, t)$ consists of both classical and quantum terms.

Eq. (16) can be solved for both TD and time-independent magnetic fields. The latter yields electronic structure for an initial ground state with $M = 0$ under static magnetic fields with varying β. Assuming the validity of Eq. (16) in imaginary time, one can transform it into a diffusion quantum Monte Carlo equation (see, e.g., [4])

$$[-\nabla^2/2 + V_{eff}(\rho;\mathbf{r},t)]R(\mathbf{r},t) = -\partial R(\mathbf{r},t)/\partial t \quad (17)$$

where $R(\mathbf{r}, t)$ is a real function such that

$$R^2(\mathbf{r},t) = \rho(\mathbf{r},t) \quad (18)$$

Eq. (17) has the same form as that for the interaction between intense laser fields and atoms or molecules. The potential V_{eff} in Eq. (17) is given by

$$V_{eff}(\rho;\mathbf{r},t) = (\delta E_{ne} + \delta E_{ee} + \delta E_x + \delta E_c + \delta E_m + \delta T_{corr})/\delta\rho \quad (19)$$

Here, the nuclear-electronic attraction potential is $-Z/r = \delta E_{ne}/\delta\rho$, where Z is the nuclear charge. E_{ee} is the classical Coulomb repulsion energy of the electrons. The exchange and correlation potentials are the Ghosh–Deb [30] and Wigner forms respectively. The exchange potential is

$$\delta E_x/\delta\rho = \delta E_x^{LDA}/\delta\rho - C_x[(4\rho^{1/3}/3) + 2r^2\rho/\alpha_x]/[1 + (r^2\rho^{2/3}/\alpha_x)]^2$$
$$\delta E_x^{LDA}/\delta\rho = -(4/3)C_x\rho^{1/3}$$
$$\alpha_x = 0.0244$$
$$C_x = (27/64\pi)^{1/3}$$

while the Wigner correlation potential is

$$\delta E_c/\delta\rho = -(a + c\rho^{-1/3})/(a + b\rho^{-1/3})^2$$

where $a = 9.81$, $b = 21.437$, and $c = 28.582667 = (4/3)b$.

Although these functionals are local ones, they yield excellent results in both static and dynamic situations involving both ground and excited states [4,31]. In Eq. (19), the last term (T_{corr}) is the kinetic energy correction term over and above the Weizsäcker kinetic energy. This vanishes identically for one-electron systems and two-electron Hartree–Fock systems. For the H_2 molecule, we neglect T_{corr}, even though our calculations yield beyond-Hartree–Fock accuracy due to the inclusion of the correlation term. In view of azimuthal symmetry, we adopt a cylindrical coordinate system and set the azimuthal angle φ as zero.

Eq. (17) is solved numerically using a finite-difference method (see [4] for details), by using the hypervirial theorem. For diatomic molecules in static magnetic fields, the hypervirial theorem can be derived as

$$2\langle T\rangle = -\langle V_0\rangle + 2\langle V_m\rangle - R\partial E/\partial R \quad (20)$$

where $\langle V_0\rangle$ is the average field-free potential energy, $\langle V_m\rangle$ is the average magnetic potential energy, $\langle T\rangle$ is the average kinetic energy, E is the total energy and R is the internuclear distance.

Let $\langle V_t\rangle = \langle V_0\rangle + \langle V_m\rangle$

Then, the hypervirial theorem takes the form

$$2 + (R/\langle T\rangle)\partial E/\partial R = -\langle V_t\rangle/\langle T\rangle + 3\langle V_m\rangle/\langle T\rangle \quad (21)$$

Note that since the potential energy curve is convex, each side (henceforth called the hypervirial) of Eq. (21) is greater than 2, for $R > R_{eq}$, the equilibrium internuclear distance; for $R = R_{eq}$, the hypervirial is exactly 2. Therefore, for each value of the magnetic field we perform the calculations with sight decrements (0.001 for each computation) in R until the hypervirial becomes $\leqslant 2.0001$. The corresponding value of R is taken as R_{eq} for that magnetic field. Then, the final calculation is performed with this R_{eq} and a simple normalized MO trial function.

The finite-difference scheme [26,27] has been employed with scaling only in the $\tilde{\rho}$ direction. This scaling is necessitated by the accumulation of electron density in a direction transverse to the magnetic field. The space and time coordinates have been discretized as follows ($\tilde{\rho}$ is along the radius and $\tilde{z}$ is along the length of the cylinder):

$$x^2 = \tilde{\rho}$$
$$x_i = \delta + ih; \quad \delta = 1\times10^{-6}; \quad i = 1,2,\ldots\ldots\ldots,N_1$$
$$\tilde{z}_k = [(N_2-1)/2 - k]h; \quad k = 1,2,\ldots\ldots\ldots..N_2$$
$$h = 0.05; \quad \Delta t = 0.0002 \text{ a.u.}; \quad N_1 = 51; N_2 = 251$$

3. Results and discussion

The essential results for the unperturbed ground $^1\Sigma_g$ state ($M = 0$, $\beta = 0$) under magnetic fields of strengths $\beta \leqslant 0.5$ are the following: As a result of the applied magnetic field, the electron density acquires an additional rotational kinetic energy due to the extra motion transverse to the direction of the magnetic field. Consequently, the density contracts towards the internuclear axis

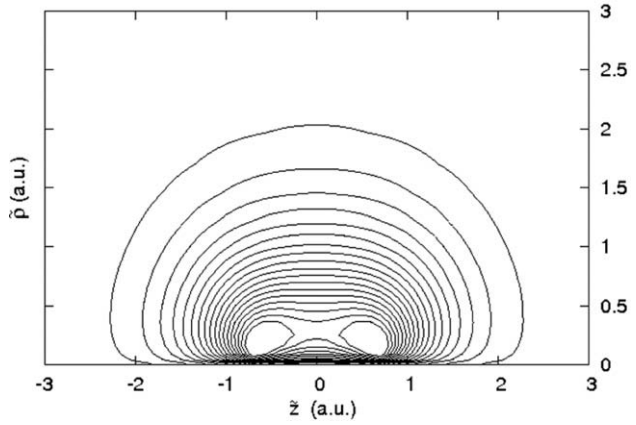

Fig. 1. Electron density contours of the H_2 molecule in the lowest $^1\Sigma_g$ state ($M = 0$) at zero magnetic field, in the $\tilde{\rho}\tilde{z}$-plane. The outermost and innermost contour values are 0.008 and 0.22, respectively. R_{eq} is 1.4 a.u.

leading to an increase in density in the binding region between the two nuclei. This strengthens the bond in this state and reduces the bond length (R_{eq}). The contraction of the density increases inter-electronic repulsion but is countered by increased electron-nuclear attraction, even though the total energy increases with an increase in β due to the increase in electronic kinetic energy caused by the additional electronic motion. The competition between the nuclear electric field and the external magnetic field is mainly responsible for the overall changes in the electron density. These conclusions are consistent with earlier works and are justified by the following diagrams.

Fig. 1 depicts a symmetric density distribution at the calculated $R_{eq} = 1.4$ a.u. and $\beta = 0$. The corresponding total energy is -1.1729 a.u. These values are in excellent agreement with the "exact" values of $R_{eq} = 1.407$ a.u. and $E = -1.17447$ a.u. [28]. This is the initial density. One can now define a difference density

$$\Delta\rho(\mathbf{r}, \beta, R_{eq}) = \rho(\mathbf{r}, \beta, R_{eq}) - \rho(\mathbf{r}, 0, 1.4) \tag{22}$$

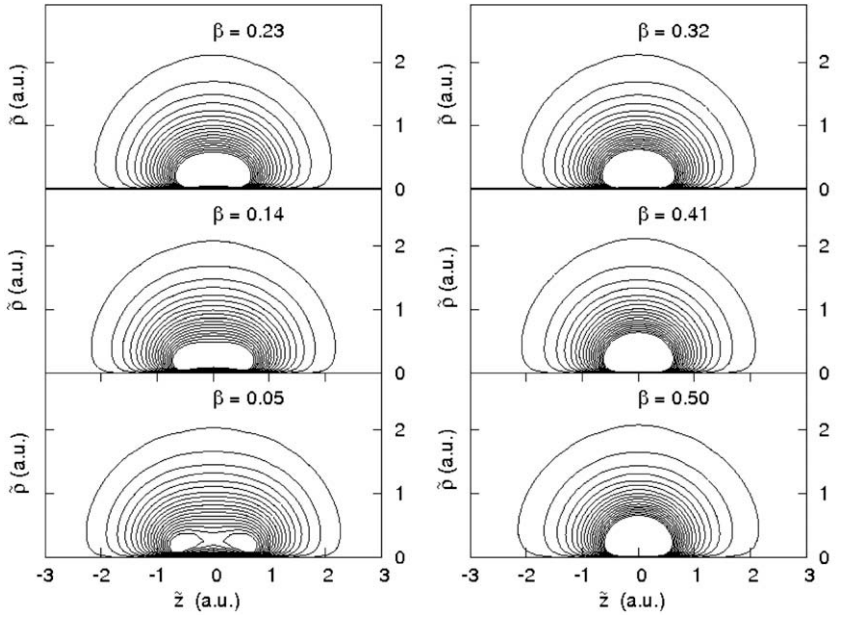

Fig. 2. Electron density contours of the H_2 molecule in the lowest $^1\Sigma_g$ state ($M = 0$) at non-zero magnetic fields, in the $\tilde{\rho}\tilde{z}$-plane, with the contour values being the same as in Fig. 1. Beginning from the lowest left panel in a clockwise direction, R_{eq} decreases progressively from the zero-field value with increasing β (see Fig. 4). The β values are given in the figure.

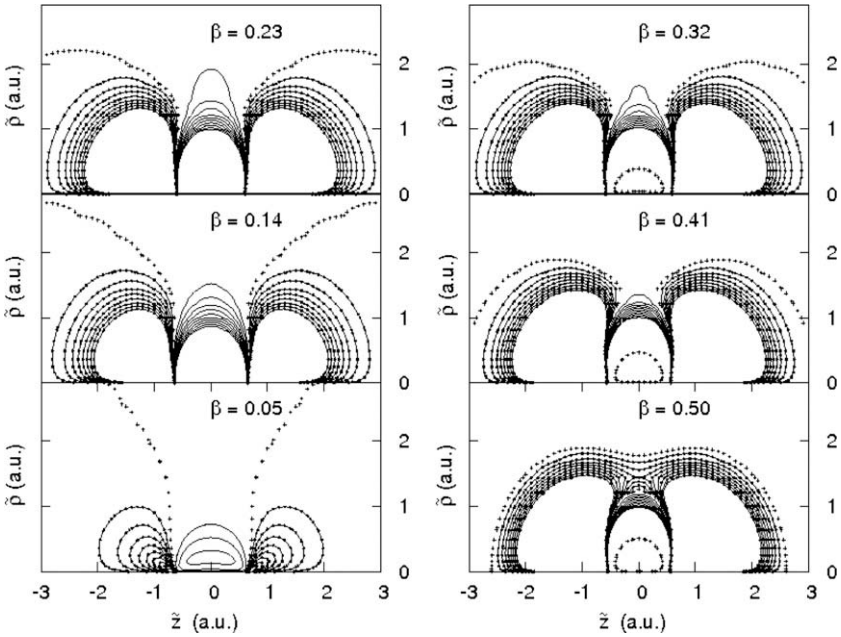

Fig. 3. Difference density contours of the H_2 molecule in the lowest $^1\Sigma_g$ state ($M = 0$) at different magnetic fields, in the $\tilde{\rho}\tilde{z}$-plane, with the same β values as the corresponding panels in Fig. 2. The solid lines denote positive $\Delta\rho$ while the barbed lines represent negative $\Delta\rho$. The dividing lines between the regions of positive and negative $\Delta\rho$ are the dotted lines signifying $\Delta\rho = 0$. For the solid lines, the outermost and innermost contour values are 0.0016 and 0.011, respectively, while the similar values for the barbed lines are -0.0032 and -0.0004. The β values are indicated in the figure.

which will show at a glance the accumulation and depletion of electron density in different regions of space [29] as a result of the external magnetic field, compared to the initial density ρ (**r**, 0, 1.4).

When the magnetic field is switched on and gradually increased in strength, the electron density contracts transverse to the direction of the field. Fig. 2 clearly shows this contraction and the resultant accumulation of electron density in the binding region between the two nuclei. However, such contraction and accumulation are more vividly depicted by the difference density plots in Fig. 3. The accumulation of electron density in the binding region leads to a shortening of bond length. This accumulation occurs due to the movement of electron density from the anti-binding regions behind the two nuclei to the binding region. Fig. 3 shows that with increasing magnetic field strength the binding region accumulates more and more electron density from the anti-binding regions, leading to a progressive shortening of the bond length. This is in complete contrast to what happens to the electron density under an intense laser electric field [4]. Therefore, it would be interesting to study the effects of both electric and magnetic fields of comparable strengths on the electron density. All density plots obtained by us show symmetry with respect to the bond mid-point. Note the gradual bending of the $\Delta\rho = 0$ lines with increasing field strength.

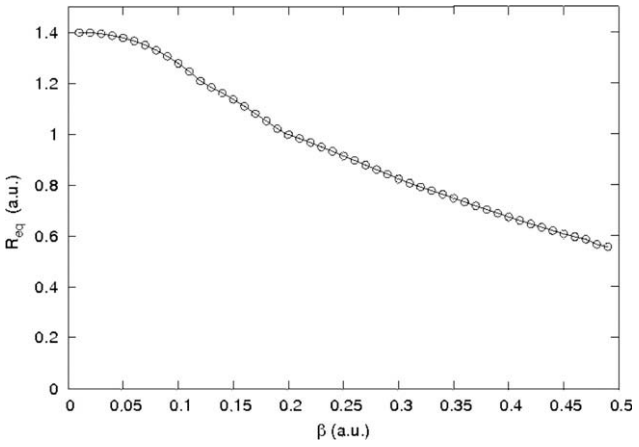

Fig. 4. The decrease of bond length (R_{eq}) in the lowest $^1\Sigma_g$ state ($M = 0$) of the H_2 molecule with increasing magnetic field.

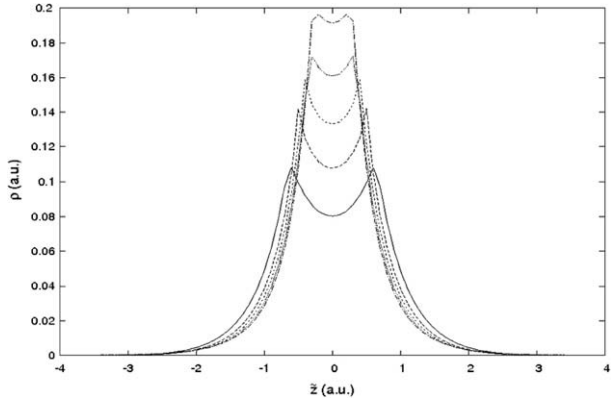

Fig. 5. Density profiles in the lowest $^1\Sigma_g$ state ($M = 0$) of the H_2 molecule showing variations of electron density cusps corresponding to nuclear positions due to increasing magnetic fields along a line parallel to the $\bar{z}$-axis and passing through the first grid point in $\bar{\rho}$ (at a distance of 0.0025 from the internuclear axis). B values from the lowest to the uppermost curve are 0.1, 0.2, 0.3, 0.4 and 0.5, respectively.

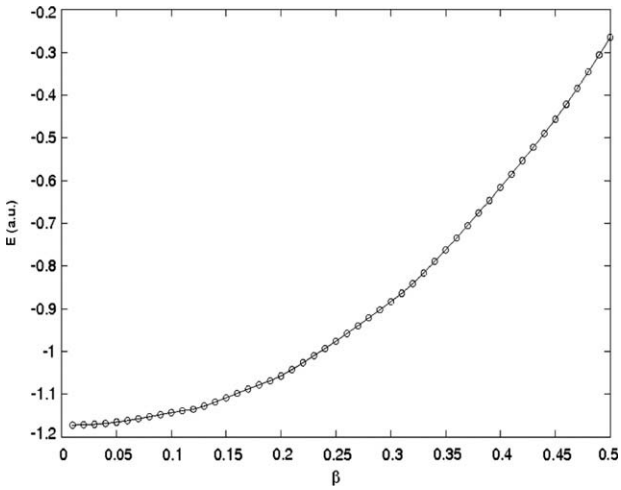

Fig. 6. Energy as a function of magnetic field, corresponding to decreasing R_{eq} with increasing field.

The decrease in bond length with increasing field strength is depicted in Fig. 4. In the initial stages (up to $\beta = 0.05$). Since H_2 has a strong chemical bond, the bond length decreases relatively slowly in the initial stages (up to $\beta = 0.05$). In the range $0.05 \leqslant \beta \leqslant 0.2$, the bond length contracts more rapidly, the rate falling off slightly for $\beta \geqslant 0.2$ for which R_{eq} varies almost linearly with β. Fig. 5 shows at a glance electron density contraction, reduction of bond length and shifting of electronic cusps corresponding to nuclear positions, due to increasing β. The increase in electronic energy as a result of increasing magnetic field, due to increasing rotational kinetic energy caused by electronic motion, is shown in Fig. 6. This increasing kinetic energy dominates over the increasing nuclear attraction energy.

4. Conclusion

In this paper we have presented additional insights into the mechanism of bond-shortening in the H_2 molecule in the lowest $^1\Sigma_g$ state ($M = 0$) due to the influence of strong magnetic fields up to a field strength of 2.3505×10^9 G. These insights accrue from visualizations of the changes in electron density in the binding and anti-binding regions of the molecule. Bond-shortening may be regarded as a consequence of the confrontation between the internal nuclear electric field and the external strong magnetic field. Since the results are consistent with those of earlier workers, it appears that the Deb–Chattaraj single equation is also suitable for studying atoms and molecules under strong magnetic fields.

Acknowledgement

M.S. thanks the C.S.I.R., New Delhi, for financial support.

References

[1] A.D. Bandrauk (Ed.), Molecules in Laser Fields, Marcel Dekker, New York, 1994.
[2] J. Itatani, J. Levesque, D. Zeidler, H. Niikura, H. Pépin, J.C. Keiffer, P.B. Corkum, D.M. Villeneuve, Nature 432 (2004) 867.
[3] X. Urbain, B. Fabre, E.M. Staicu-Casagrande, N. de Ruette, V.M. Andrianarijaona, J. Jureta, J.H. Posthumus, A. Saenz, E. Baldit, C. Cornaggia, Phys. Rev. Lett. 92 (2004) 163004.
[4] A. Wadehra, B.M. Deb, Eur. Phys. J. D 39 (2006) 141.
[5] D. Lai, Rev. Mod. Phys. 73 (2001) 629.
[6] T.O. Klaassen, J.L. Dunn, C.A. Bates, in: P. Schmelcher, W. Schweizer (Eds.), Atoms and Molecules in Strong Magnetic Fields, Plenum, New York, 1998.
[7] V.M. Kaspi, D. Chakrabarty, J. Steinberger, Astrophys. J. 525 (1999) L33.
[8] U. Kappes, P. Schmelcher, Phys. Rev. A 54 (1996) 1313.
[9] Y.P. Kravchenko, M.A. Liberman, Phys. Rev. A 55 (1997) 2701.

[10] A.V. Korolev, M.A. Liberman, Phys. Rev. Lett. 72 (1994) 270.
[11] D. Lai, Phys. Rev. Lett. 74 (1995) 4095.
[12] M. Farconi, G. Vignale, Phys. Rev. B 50 (1994) 14722.
[13] B.M. Relovsky, H. Ruder, Phys. Rev. A 53 (1996) 4068.
[14] G. Ortiz, M.D. Jones, D.M. Ceperly, Phys. Rev. A 52 (1995) R3405.
[15] T. Detmer, P. Schmelcher, F.K. Diakonos, L.S. Cederbaum, Phys. Rev. A 56 (1997) 1825.
[16] T. Detmer, P. Schmelcher, L.S. Cederbaum, Phys. Rev. A 57 (1998) 1767.
[17] Y.P. Kravchenko, M.A. Liberman, Phys. Rev. A 56 (1997) R2510.
[18] P. Schmelcher, L.S. Cederbaum, Phys. Rev. A 37 (1988) 672.
[19] B.M. Deb, P.K. Chattaraj, Phys. Rev. A 39 (1989) 1696.
[20] B.M. Deb, S.K. Ghosh, J. Phys. B: At. Mol. Phys. 12 (1979) 3857.
[21] S.K. Ghosh, B.M. Deb, Phys. Rep. 92 (1982) 1.
[22] B.M. Deb, S.K. Ghosh, J. Chem. Phys. 77 (1982) 342.
[23] L.J. Bartolotti, Phys. Rev. A 24 (1981) 1661.
[24] E. Runge, E.K.U. Gross, Phys. Rev. Lett. 52 (1984) 997.
[25] S.K. Ghosh, A.K. Dhara, Phys. Rev. A 38 (1988) 1149.
[26] A.K. Roy, B.K. Dey, B.M. Deb, Chem. Phys. Lett. 308 (1999) 523.
[27] A. Poddar, B.M. Deb, J. Phys. A: Math. Theor. 40 (2007) 5981.
[28] W. Kolos, L. Wolniewicz, J. Chem. Phys. 43 (1965) 2429.
[29] R.F.W. Bader, in: B.M. Deb (Ed.), The Force Concept in Chemistry, Van Nostrand-Reinhold, New York, 1981.
[30] S.K. Ghosh, B.M. Deb, J. Phys. B: At. Mol. Opt. Phys. 27 (1994) 381.
[31] R. Singh, B.M. Deb, Phys. Rep. 311 (1999) 47.